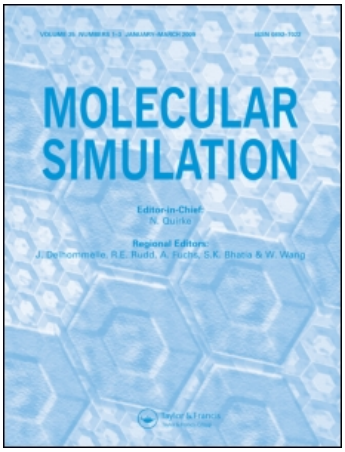

Molecular Simulation
Publication details, including instructions for authors and subscription information:
http://www.informaworld.com/smpp/title~content=t713644482

Direct Evaluation of Vapour-Liquid Equilibria of Mixtures by Molecular Dynamics Using Gibbs-Duhem Integration

Martin Lísal[a]; Václav Vacek[b]
[a] E. Hála Laboratory of Thermodynamics, Institute of Chemical Process Fundamentals, Academy of Sciences, Prague 6, Czech Republic [b] Department of Physics, Czech Technical University, Prague 6, Czech Republic

To cite this Article Lísal, Martin and Vacek, Václav(1996) 'Direct Evaluation of Vapour-Liquid Equilibria of Mixtures by Molecular Dynamics Using Gibbs-Duhem Integration', Molecular Simulation, 18: 1, 75 — 99
To link to this Article: DOI: 10.1080/08927029608022355
URL: http://dx.doi.org/10.1080/08927029608022355

Molecular Simulation, 1996, Vol. 18, pp. 75–99
Reprints available directly from the publisher
Photocopying permitted by license only

DIRECT EVALUATION OF VAPOUR-LIQUID EQUILIBRIA OF MIXTURES BY MOLECULAR DYNAMICS USING GIBBS-DUHEM INTEGRATION

MARTIN LÍSAL[a] and VÁCLAV VACEK[b]

[a]*E. Hála Laboratory of Thermodynamics, Institute of Chemical Process Fundamentals, Academy of Sciences, 165 02 Prague 6, Czech Republic*
[b]*Department of Physics, Czech Technical University, 167 06 Prague 6, Czech Republic*

(Received March 1996; accepted March 1996)

We present an extension of the Gibbs-Duhem integration method that permits direct evaluation of vapour-liquid equilibria of mixtures by molecular dynamics. The Gibbs-Duhem integration combines the best elements of the Gibbs ensemble Monte Carlo technique and thermodynamic integration. Given conditions of coexistence of pure substances, simultaneous but independent molecular dynamics simulations of each phase at constant number of particles, constant pressure, constant temperature and constant fugacity fraction of species 2 are carried out in succession along coexistence lines. In each simulation, the coexistence pressure is adjusted to satisfy the Clapeyron-type equation. The Clapeyron-type equation is a first-order nonlinear differential equation that prescribes how the pressure must change with the fugacity fraction of species 2 to maintain coexistence at constant temperature. The Clapeyron-type equation is solved by the predictor-corrector method. Running averages of mole fraction and compressibility factor for the two phases are used to evaluate the right-hand side of the Clapeyron-type equation. The Gibbs-Duhem integration method is applied to three prototypes of binary mixtures of the two-centre Lennard-Jones fluid having various elongations. The starting points on the coexistence curve were taken from published data.

Keywords: Vapour-liquid equilibria; Gibbs-Duhem method; Clapeyron equation; 2 centre LJ's fluid

1. INTRODUCTION

The calculation of vapour-liquid equilibria (VLE) for macroscopic systems from knowledge of molecular interactions is one of the central goals of statistical thermodynamics. Undoubtely, the Panagiotopoulos Gibbs

ensemble Monte Carlo (GEMC) method [1, 2] is the most popular technique for the direct evaluation of VLE. It enables us with a single simulation to locate and evaluate the coexistence conditions for a given system. The GEMC involves (a) setting-up a two-phase thermodynamic system with no physical contact between the two regions and no interface, and (b) three simulation steps necessary to satisfy the conditions of thermodynamic equilibrium. Thermodynamic equilibrium requires that temperature, pressure and chemical potential (fugacity) of all components have to be the same in both regions. In the GEMC methodology, the equality of temperature, pressure and chemical potential (fugacity) of all components corresponds to displacement, volume-change and particle-insertion simulation steps, respectively. The GEMC technique suffers from certain limitations due to particle-exchange moves. Problems inherent in the particle insertion method occur at high densities [3]. Moreover, drawbacks of the GEMC arise when it is applied to systems modelled by complex intermolecular potentials, unless special procedures are employed [4].

Recently, Kofke [5, 6] has proposed a new method for the direct evaluation of phase coexistence by molecular simulations: the Gibbs-Duhem integration. He utilized the Monte Carlo (MC) method and applied the Gibbs-Duhem integration to the Lennard-Jones fluid [5, 6] and to the Lennard-Jones binary mixtures [7, 8]. The application of the Gibbs-Duhem integration by molecular dynamics (MD) to molecular fluid has been described by Lisal and Vacek [9]. The Gibbs-Duhem integration combines the best features of the GEMC technique and thermodynamic integration. The method entails simultaneous simulations of each phase (as does the GEMC method) either at constant number of particles, constant pressure and constant temperature (NPT) for pure substances or at constant number of particles, constant pressure, constant temperature and constant fugacity fraction of species 2 (NPTζ_2) [7] for mixtures. The mechanism for equating the chemical potential (fugacity) is the Clapeyron-type equation. Hence, in contrast to the GEMC method, no particle insertion is necessary in the case of pure substances. In the case of mixtures, the NPTζ_2 simulation requires change of species indentity. The change of species indentity works much more efficiently than particle insertion. However, the change of species indentity can also fail while dealing with species that differ significantly in their size and interaction parameters. Starting at a state point for which the two phases of one of the pure substances are known to be in equilibrium, the Gibbs-Duhem integration method can be used to trace out the phase diagram directly and efficiently.

Following on from our previous work [9], we applied the Gibbs-Duhem integration method to the three prototypes of binary mixtures of two-centre

Lennard-Jones (2CLJ) fluid having elongations of 0.3292, 0.505 and 0.67. We chose 2CLJ fluids because their VLE has recently been determined from the NPT plus test particle method [11]. In contrast to Kofke [7], who utilized the MC method, we carried out the NPTζ_2 simulations by the MD method. The MD method has advantages over the MC method in that dynamical properties can be assessed. Section 2 presents the Clapeyron-type equations. Section 3 gives the 2CLJ potential, MD algorithm for carrying the NPTζ_2 simulations and simulation details. Section 4 presents results of the Gibbs-Duhem integration for three prototypes of molecular binary mixtures. Finally, our conclusions are summarized in Section 5.

2. CLAPEYRON-TYPE EQUATIONS

The semigrand form of the Gibbs-Duhem equation for binary mixtures [7] can be written as

$$d\ln(f_1+f_2) = h_r d\beta + Z d\ln p - \frac{x_2-\zeta_2}{\zeta_2(1-\zeta_2)} d\zeta_2. \tag{1}$$

In Eq. (1), p is the pressure, and Z is the compressibility factor, $p\beta/\rho$, where ρ is the number density, $\beta = 1/k_B T$, with k_B the Boltzmann constant and T the temperature; x_i is the mole fraction of species i with fugacity f_i, and ζ_2 is the fugacity fraction of species 2; h_r is the residual enthalpy, defined as the enthalpy above an ideal gas at the same temperature. The fugacity fraction [10] of species 2

$$\zeta_2 = \frac{f_2}{f_1+f_2} \tag{2}$$

is a convenient quantity that varies from zero to unity as mixtures change from pure species 1 to pure species 2. Both ζ_2 and the sum (f_1+f_2) must have the same values in two coexisting phases. Clapeyron-type equations are derived by considering variations in temperature, pressure, and fugacity fraction of species 2 that keep changes in the sum (f_1+f_2) equal between phases [12]. The following formula [7] results in

$$(h_r^l - h_r^v)\, d\beta + (Z^l - Z^v)\, d\ln p - \left[\frac{x_2^l - x_2^v}{\zeta_2(1-\zeta_2)}\right] d\zeta_2 = 0 \tag{3}$$

The Clapeyron-type equation for variations at constant temperature derived from Eq. (3) becomes

$$\left(\frac{\partial \ln p}{\partial \zeta_2}\right)_{\beta,\sigma} = \frac{x_2^l - x_2^v}{\zeta_2(1-\zeta_2)(Z^l - Z^v)} \tag{4}$$

and the equation for variations at constant pressure is

$$\left(\frac{\partial \beta}{\partial \zeta_2}\right)_{p,\sigma} = \frac{x_2^l - x_2^v}{\zeta_2(1-\zeta_2)(h_r^l - h_r^v)}, \tag{5}$$

where the subscript σ indicates that the derivative is taken along the coexistence line.

The right-hand side of Eqs. (4,5) is no longer defined at limits $x_2 \to 0$ and $x_2 \to 1$. Approaching those limits, the fugacity of the dilute component obeys Henry's Law, while the abundant species obeys Rauolt's Law. At the limit $x_2 \to 0$, Eq. (4) and Eq. (5) [7] have the form

$$\left(\frac{\partial \ln p}{\partial \zeta_2}\right)_{\beta,\sigma} = \frac{f_1^0/H_2^l - f_1^0/H_2^v}{Z^l - Z^v} \tag{6}$$

$$\left(\frac{\partial \beta}{\partial \zeta_2}\right)_{p,\sigma} = \frac{f_1^0/H_2^l - f_1^0/H_2^v}{h_r^l - h_r^v}, \tag{7}$$

respectively. Similarly, at the limit $x_2 \to 1$, Eq. (4) and Eq. (5) [7] result in

$$\left(\frac{\partial \ln p}{\partial \zeta_2}\right)_{\beta,\sigma} = -\frac{f_2^0/H_1^l - f_2^0/H_1^v}{Z^l - Z^v} \tag{8}$$

$$\left(\frac{\partial \beta}{\partial \zeta_2}\right)_{p,\sigma} = -\frac{f_2^0/H_1^l - f_2^0/H_1^v}{h_r^l - h_r^v}, \tag{9}$$

respectively. In Eqs.(6–9), H_i is the Henry's constant, and f_j^0 is the fugacity of pure component j at the temperature of the mixture and at its coexistence pressure. Ratios f_j^0/H_i can be evaluated in pure-solvent simulations by performing trial identity changes. The ratio f_j^0/H_i is then given as

$$\frac{f_j^0}{H_i} = \langle \exp(-\beta \Delta u) \rangle, \tag{10}$$

where Δu is the exchange energy.

Given an initial condition, *i.e.*, the pressure, temperature, density, residual enthalpy and ratio f_j^0/H_i of one of the pure components, Eqs. (4, 5) can be solved numerically by a predictor-corrector method [6, 7, 9]. The right-hand side of Eqs. (4, 5) is computed by the MD method having as independent variables the total number of molecules N, the pressure P, the temperature T and the fugacity fraction of species 2 ζ_2. Eq. (4) results in a pressure-composition diagram P-x_2, while Eq. (5) results in a temperature-composition diagram T-x_2.

3. SIMULATION METHOD

3.1. Intermolecular potential

We applied the Gibbs-Duhem integration method to mixtures of 2CLJ fluids having various elongations l. The pair potential for 2CLJ fluid is

$$u_{2\mathrm{CLJ}}(r,\omega_i,\omega_j) = \sum_{a=1}^{2}\sum_{b=1}^{2} 4\varepsilon\left[\left(\frac{\sigma}{r_{ab}}\right)^{12} - \left(\frac{\sigma}{r_{ab}}\right)^{6}\right]. \tag{11}$$

In Eq. (11), r_{ab} is the distance between atom a of molecule i and atom b of molecule j, ε and σ are the Lennard-Jones energy and size parameters, and ω is the orientation of the molecules. In the following, we used the Lennard-Jones reduced units: $L = l/\sigma, r^* = r/\sigma, t^* = t/(\sigma\sqrt{(m/\varepsilon)})$, $T^* = k_B T/\varepsilon, \rho^* = \rho\sigma^3$, $p^* = P\sigma^3/\varepsilon$, $h^* = h/N\varepsilon$, and $Z = p^*/\rho^* T^*$.

3.2. NPT ζ_2 MD algorithm

The Gibbs-Duhem integration method for mixtures requires us to carry out MD simulations at constant number of particles N, constant pressure P constant temperature T and constant fugacity fraction of species 2 ζ_2. The temperature was kept constant by isokinetic scaling of the centre-of-mass (COM) and angular velocities after every timestep. The constant pressure P was maintained by weak coupling to an external bath of constant pressure [13]. This represents a proportional scaling of COM coordinates and box length every timestep by the pressure scaling factor

$$\mu = \left[1 + \frac{\Delta t}{\tau_P}\chi_T(\mathscr{P} - P)\right]^{1/3}. \tag{12}$$

Here, $\mathscr{P}$ is the instantaneous pressure, τ_P is the time constant of the pressure coupling, Δt is the timestep and ξ_T is the isothermal compressibility.

We combined the methods proposed by Kofke and Glandt [10], and Vega *et al.* [14] to maintain a constant fugacity fraction of species $2\,\zeta_2$. After every NPT MD timestep, a molecule was choosen at random and an attempt was made to change its identity. The change of the molecule identity involved interchanging size and interaction parameters of molecules, but did not alter their COM positions and orientations. The change of the molecule identity was accepted with the average probability [10, 14]

$$\mathscr{P}_{\text{change of identity}} = \min\left[1, \left(\frac{\zeta_2}{1-\zeta_2}\right)^m \langle \exp(-\beta \Delta u) \rangle_{(N_1, N_2)}\right]. \tag{13}$$

In Eq. (13), N_i is the number of particles of species i, Δu is the change of energy due to identity change, $m = -1$ for identity change from species 2 to species 1, and $m = +1$ otherwise.

3.3. Simulation details

All simulation runs were performed with 256 molecules in a cubic box. The equations of translational motion were solved by the Gear predictor-corrector algorithm of the fifth order. The rotational motion was treated by the method of quaternions and it was solved by the Gear predictor-corrector algorithm of the fourth order [3]. The minimum image convention, periodic boundary conditions and cut-off radius equal to the half-box length were used. Long-range corrections of the internal energy and pressure were included [3]. For the integration, the timestep $\Delta t^* = 1.5 \cdot 10^{-3}$ was chosen. The isothermal compressibility χ_T was set to 1 for the liquid and 10 for the vapour, and τ_P was equal to 0.3.

We used Eqs. (4, 6, 8) to compute the VLE of binary mixtures in the $p^* - x_2$ projection of the coexistence surface along the isotherms. We proceeded with the Gibbs-Duhem integration method as follows: Starting from fcc lattices, we performed the pure-solvent NVT MD simulations of liquid and vapour phases at the coexistence points and determined the quantities needed in Eqs. (6, 8). This follows by the NPTζ_2 MD simulations. At each fugacity fraction of species 2, the simulations of the liquid and vapour phases were performed simultaneously but independently. The fugacity fraction of species 2 was increased and the predictor pressure was calculated. Afterwards, the liquid and vapour structures were allowed to relax 4000 timesteps. At the end of the relaxation period, all accumulators were set to

zero. The subsequent production run of the liquid and vapour phases was divided into nine timeblocks. The first timeblock consisted of 4000 timesteps and the following timeblocks contained 2000 timesteps each. After each timeblock was completed, the computed running averages of liquid and vapour mole fraction, and liquid and vapour compressibility factor, were used to evaluate the right-hand side of the Clapeyron-type equation: Eq. (4), and thus, to calculate the corrector pressure. Then, the fugacity fraction of species 2 was again increased and the process was repeated. The predictor and corrector pressures were evaluated according to appropriate equations given in [6, 7, 9]. The fugacity fraction of species 2 was increased in constant steps $\Delta\zeta_2$ of 0.05 or 0.025. Standard deviations were calculated by dividing the particular simulation runs into several blocks comprising 1000 consecutive steps.

4. RESULTS AND DISCUSSION

We applied the Gibbs-Duhem integration method in order to evaluate VLE along isotherms for three prototypes of binary mixtures of 2CLJ fluids having elongations 0.3292, 0.505 and 0.67. Critical parameters of the 2CLJ fluids are summarized in Table I [11] and parameters for each mixture studied are listed in Table II.

We started the Gibbs-Duhem integration from pure component 1. The starting coexistence data were taken from Kriebel *et al.* [11] or were

TABLE I Critical pressure p_C^*, critical temperature T_C^*, critical density ρ_C^* and critical compressibility factor Z_C for the two-centre Lennard-Jones fluid of elongations $L = 0.3292$, 0.505 and 0.67 [11]

L	p_C^*	T_C^*	ρ_C^*	Z_C
0.3292	0.2839	3.5436	0.24524	0.327
0.505	0.1881	2.8001	0.20566	0.327
0.670	0.1367	2.3355	0.17526	0.334

TABLE II Model parameters for mixtures studied

Mixture	L_1	L_2	σ_{11}	σ_{12}	σ_{22}	ε_{11}	ε_{12}	ε_{22}
I	0.505	0.3292	1.0	1.0	1.0	1.0	1.0	1.0
II	0.505	0.67	1.0	1.0	1.0	1.0	1.0	1.0
III	0.505	0.505	1.0	1.0	1.0	1.0	0.75	1.0

determined by pure-solvent NVT MD simulations. The data are presented in Table III.

The temperature of mixture I is subcritical for both components. Figure 1a presents the plot of $p^* - \zeta_2$ which corresponds to the solution of the Clapeyron-type equation. The pressure p^* is a smooth and slow-varying function of ζ_2, and thus, the Gibbs-Duhem integration posed no difficulties. The pressure-composition projection of the coexistence surface has the familiar spindle shape, and it is shown in Figure 1b. The result pressure at

TABLE III Starting coexistence data of the Gibbs-Duhem integration taken from Kriebel *et al.* [11] and determined by pure-solvent NVT MD simulations (denoted by †).

Mixture	T^*	ρ_v^*	ρ_l^*	p_σ^*	H_2^v/f_1^0	H_2^l/f_1^0
I	2.55	0.0672(17)	0.3618(16)	0.1105(18)	0.890(18)†	0.537(21)†
II	2.35	0.0372(8)	0.4120(7)	0.0652(10)	1.054(6)†	1.906(20)†
III	2.35	0.0372(8)	0.4120(7)	0.0652(10)	1.259(19)†	7.542(26)†
	2.45	0.0507(15)	0.3883(10)	0.0855(15)	1.330(15)†	6.131(23)†
	2.55	0.0672(17)	0.3618(16)	0.1105(18)	1.434(17)†	5.021(57)†

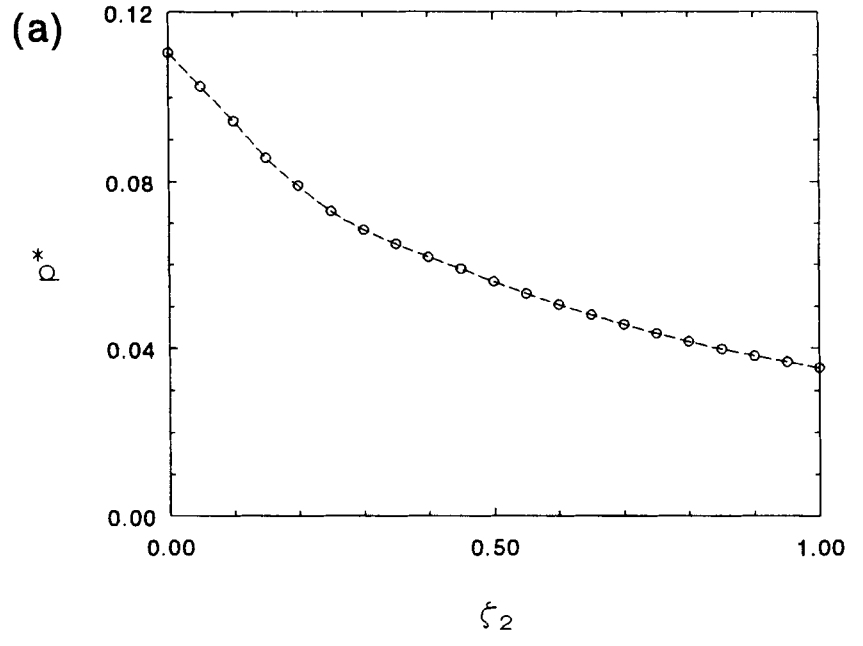

FIGURE 1

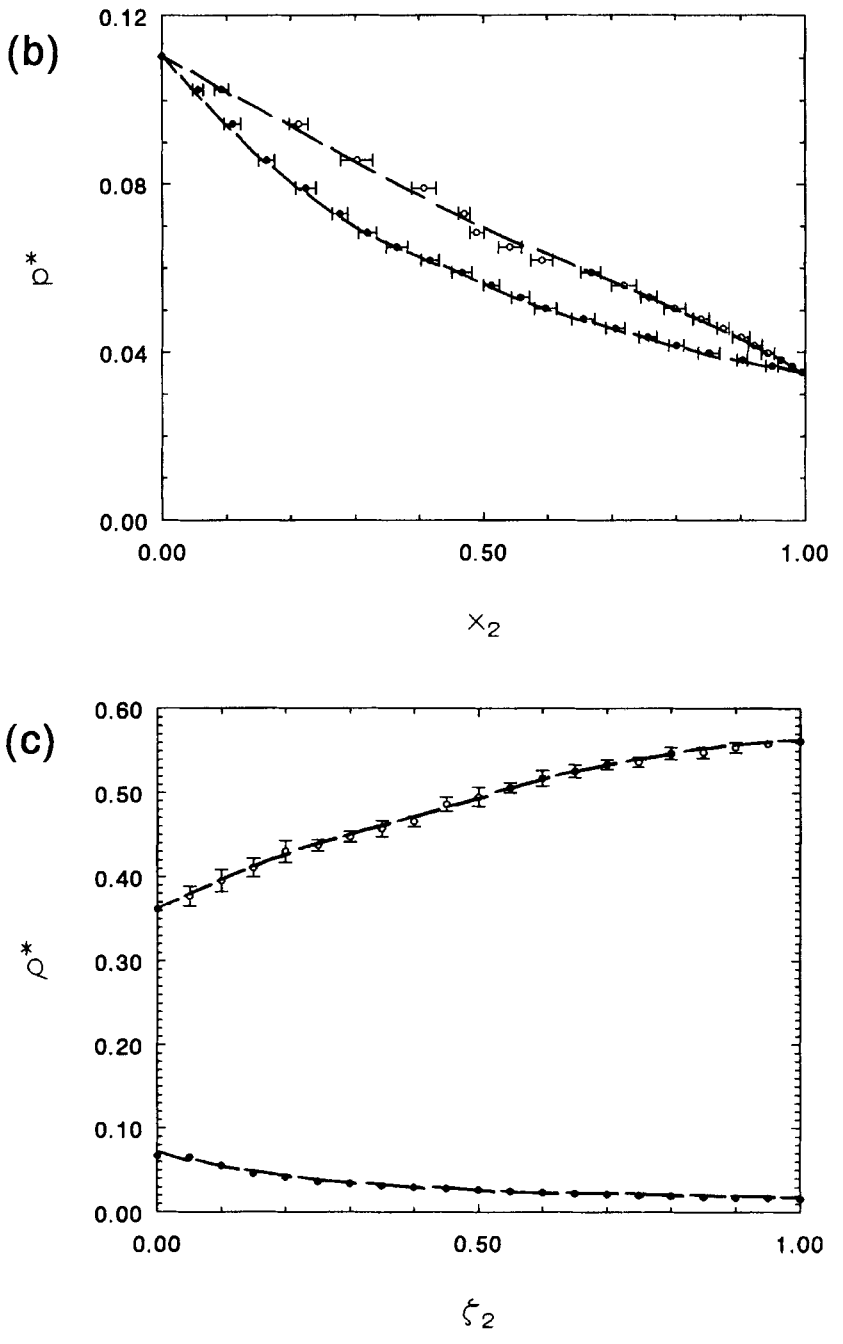

FIGURE 1

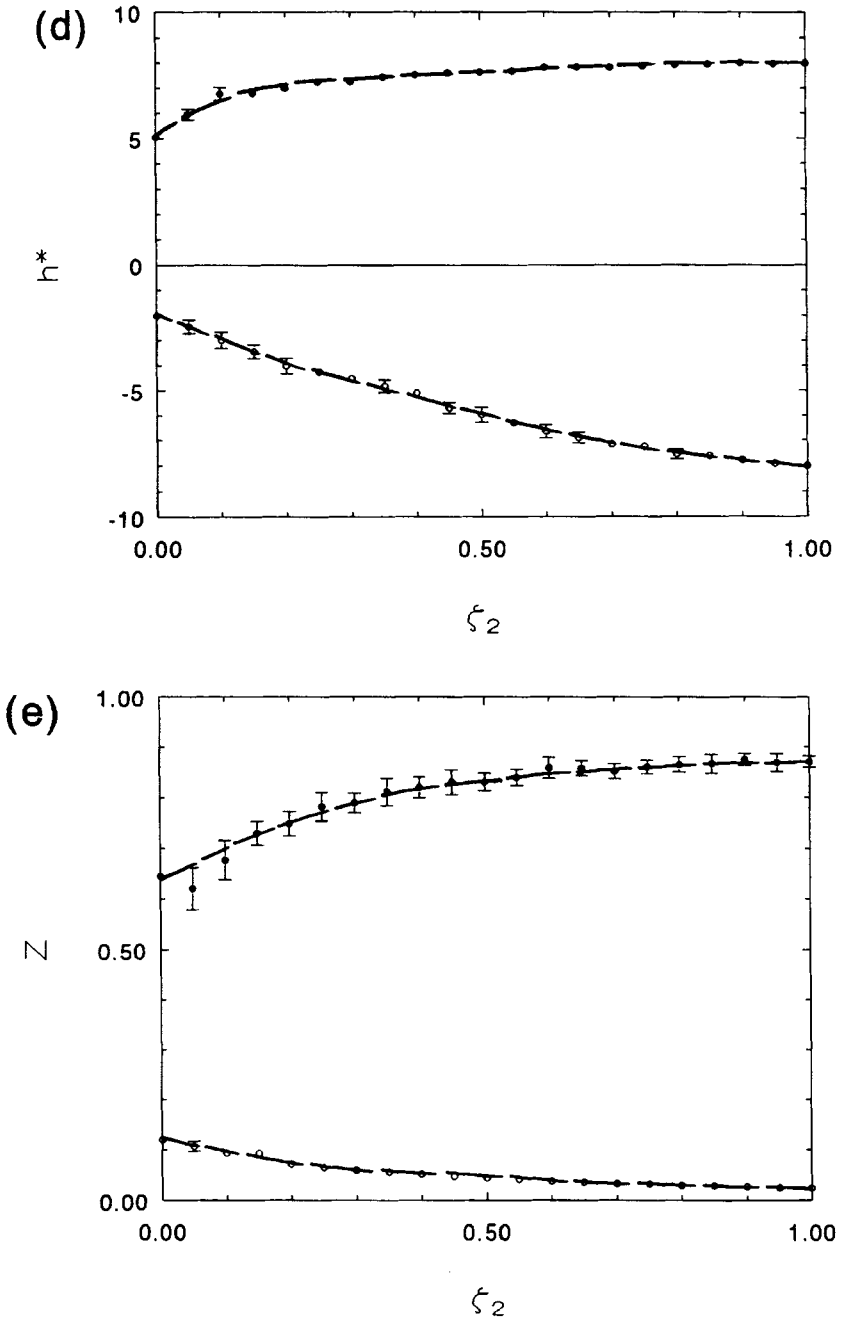

FIGURE 1

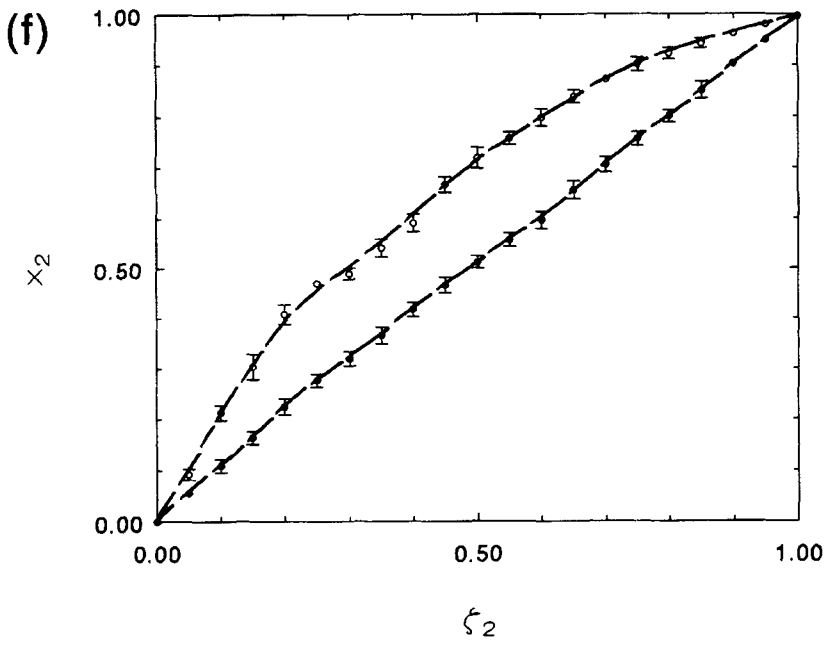

FIGURE 1 Vapour-liquid coexistence diagrams for mixture I at reduced temperature 2.55. (a) Pressure p^* as a function of fugacity fraction of species 2 ζ_2 (o: the Gibbs-Duhem integration path); (b) Pressure p^* as a function of mole fraction of species 2 x_2 (●: vapour boundary, o: liquid boundary); (c) Coexistence densities p^* as a function of fugacity fraction of species 2 ζ_2 (●: vapour boundary, o: liquid boundary); (d) Coexistence residual enthalpies h^* as a function of fugacity fraction of species 2 ζ_2 (●: vapour boundary, o: liquid boundary); (e) Coexistence compressibility factors Z as a function of fugacity fraction of species 2 ζ_2 (●: vapour boundary, o: liquid boundary); (f) Coexistence mole fraction x_2 as a function of fugacity fraction of species 2 ζ_2 (●: vapour boundary, o: liquid boundary). Error bars are included only if larger than the plot marks. Dashed lines on the phase boundaries are drawn only as a guide to the eye.

$x_2 = 1$ is the same (within its statistical uncertainties) as the coexistence pressure of pure component 2 [11]. The ratios H_1^v/f_2^0 and H_1^l/f_2^0 computed by the pure-solvent NVT MD simulations and needed in Eq. (8) are 1.027 (7) and 3.347(97), respectively. Figures 1c–f display other coexistence quantities, namely ρ^*, h^*, Z and x_2, as a function of ζ_2.

Component 2 of mixture II is supercritical, so the coexistence line must terminate at a critical point. Figure 2a shows the plot of $p^* - \zeta_2$. One can see in Figure 2a that as the critical point is approached, the pressure p^* rises steeply after a period of slow increase. The pressure-composition projection is terminated at $x_2 \sim 0.85$ as is seen in Figure 2b. As the transition weakens upon approach to the critical point, differences in the properties of the two

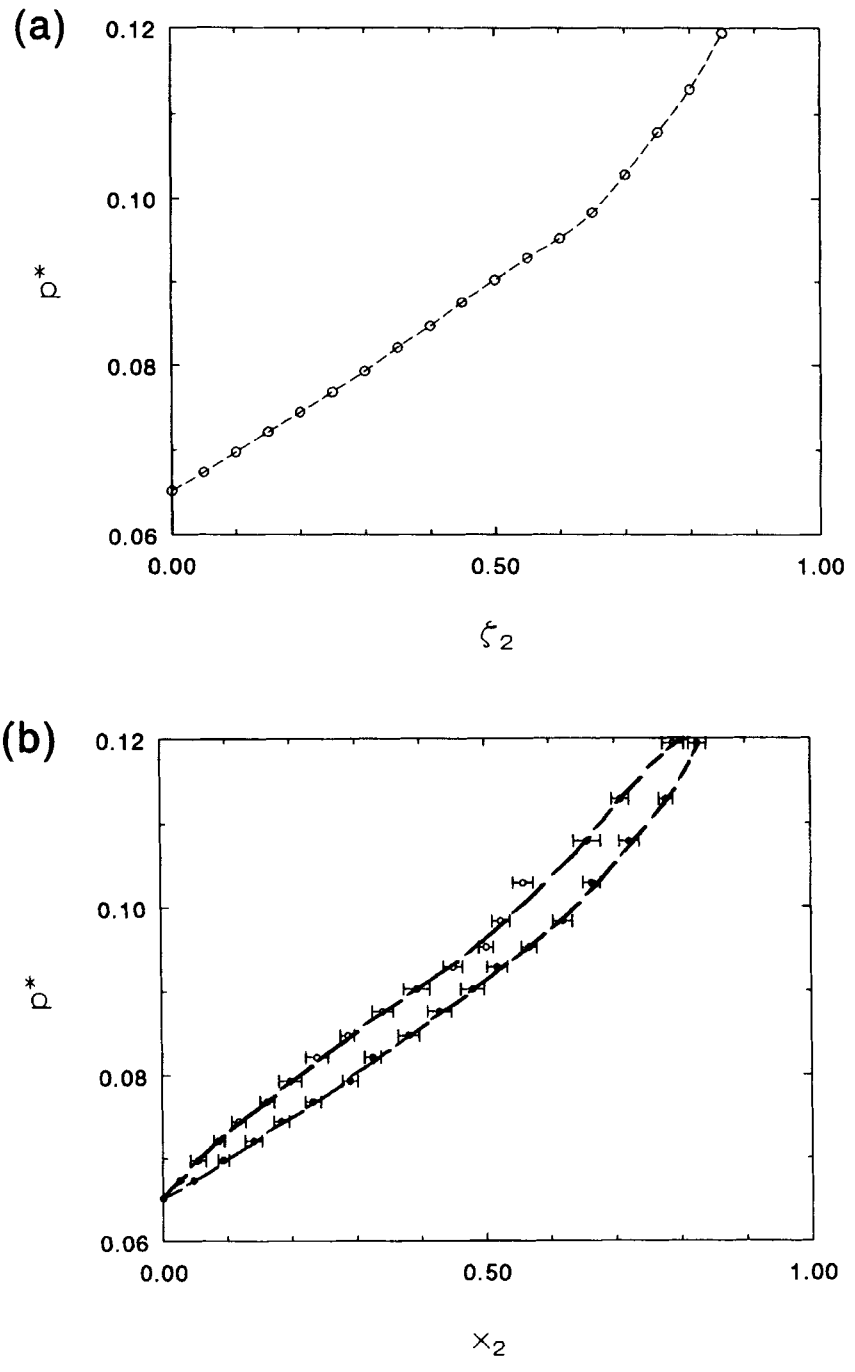

FIGURE 2

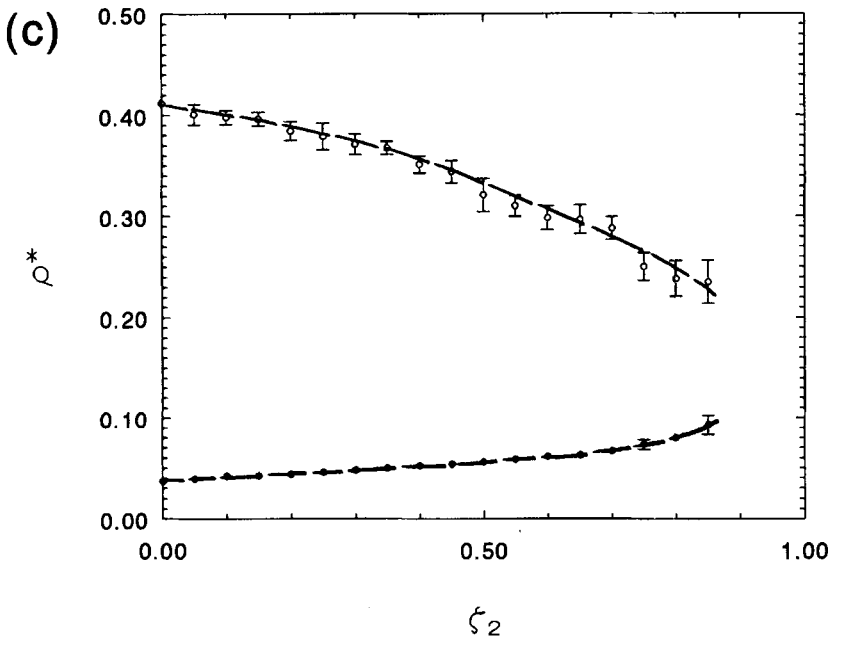

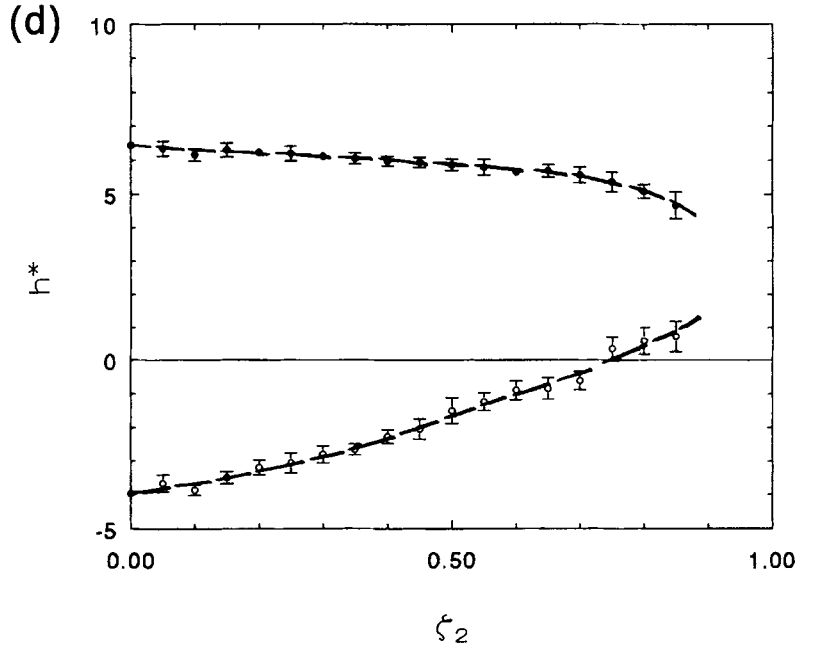

FIGURE 2

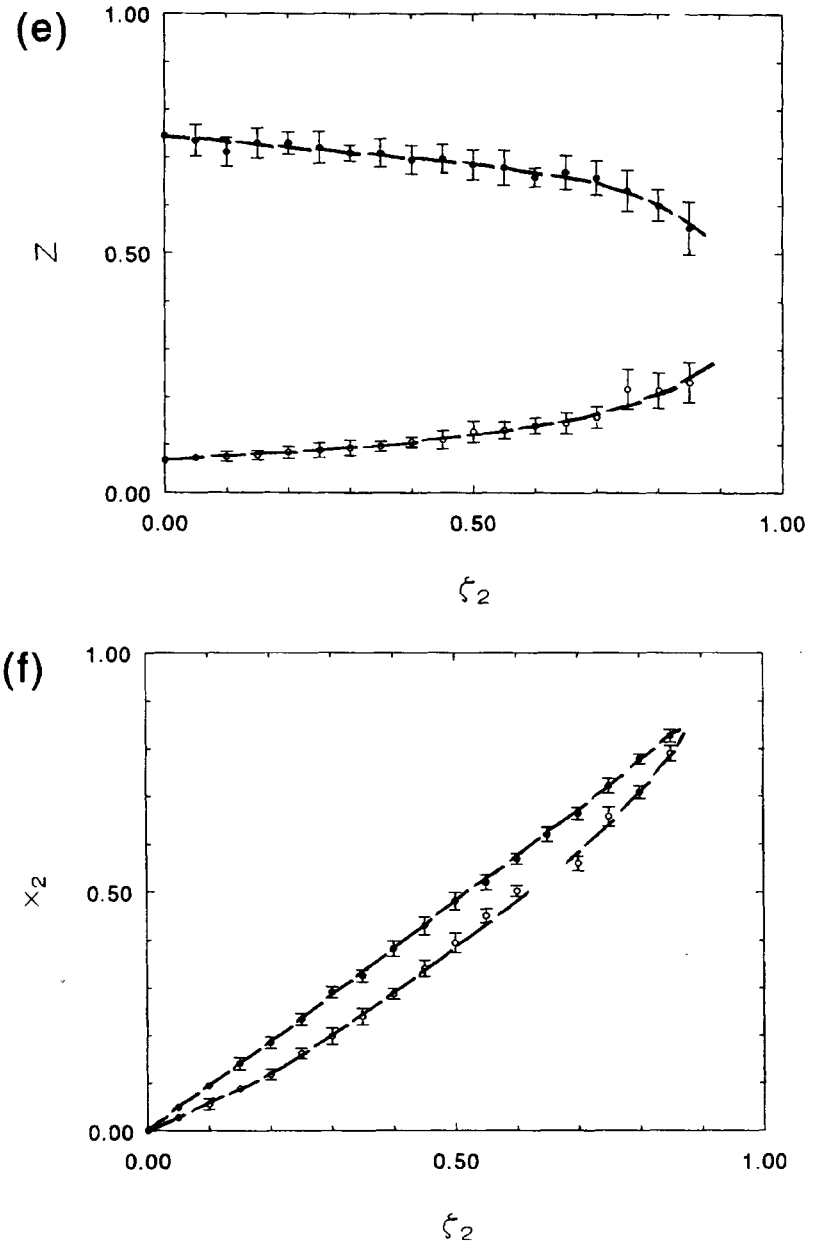

FIGURE 2 Vapour-liquid coexistence diagrams for mixture II at reduced temperature 2.35. (a) Pressure p^* as a function of fugacity fraction of species 2 ζ_2 (o: the Gibbs-Duhem integration path). (b) Pressure p^* as a function of mole fraction of species 2 x_2 (●: vapour boundary, o: liquid boundary). (c) Coexistence densities p^* as a function of fugacity fraction of species 2 ζ_2 (●: vapour boundary, o: liquid boundary); (d) Coexistence residual enthalpies h^* as a function of fugacity fraction of species 2 ζ_2 (●: vapour boundary, o: liquid boundary); (e) Coexistence compressibility factors Z as a function of fugacity fraction of species 2 ζ_2 (●: vapour boundary, o: liquid boundary); (f) Coexistence mole fraction x_2 as a function of fugacity fraction of species 2 ζ_2 (●: vapour boundary, o: liquid boundary). Error bars are included only if larger than the plot marks. Dashed lines on the phase boundaries are drawn only as a guide to the eye.

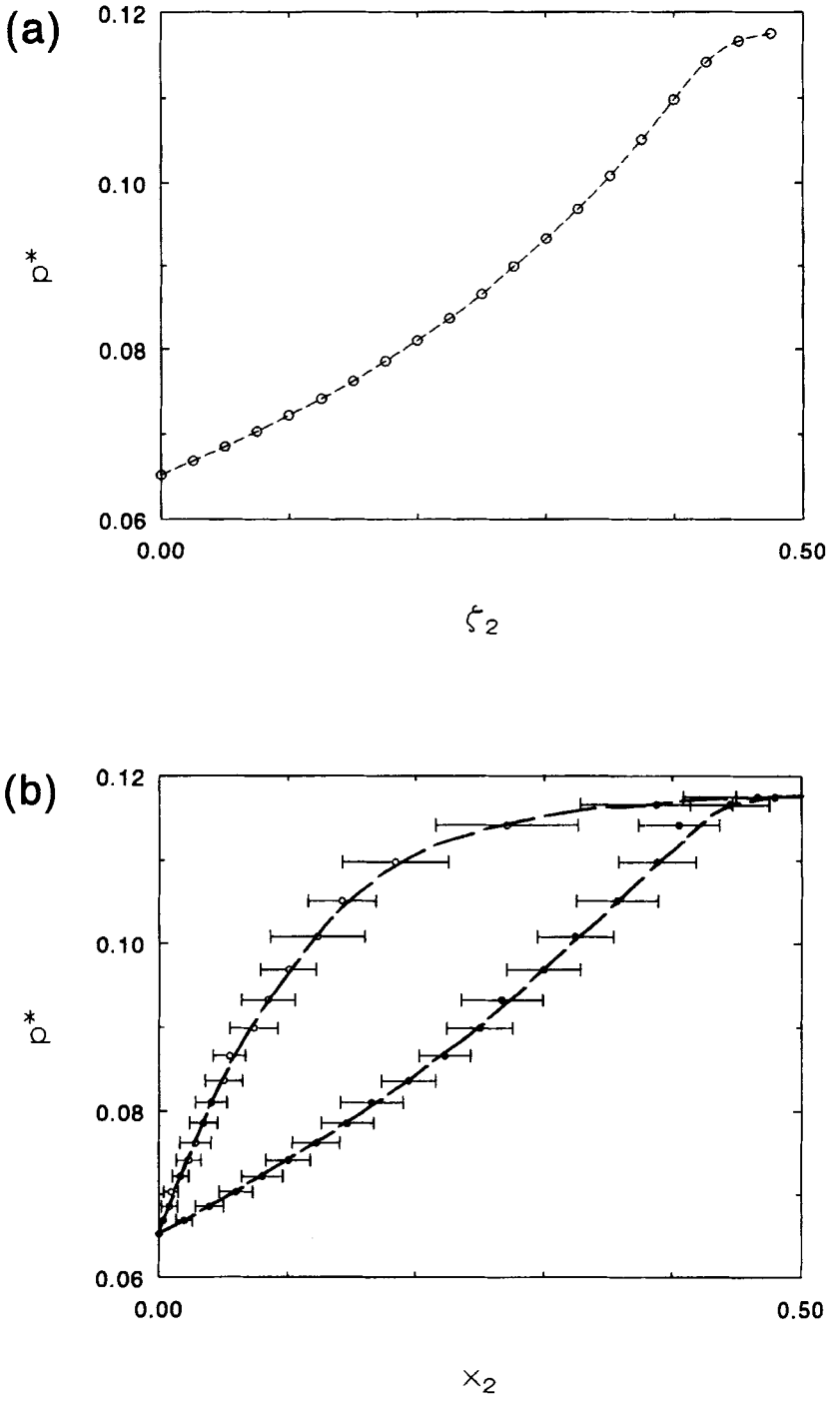

FIGURE 3

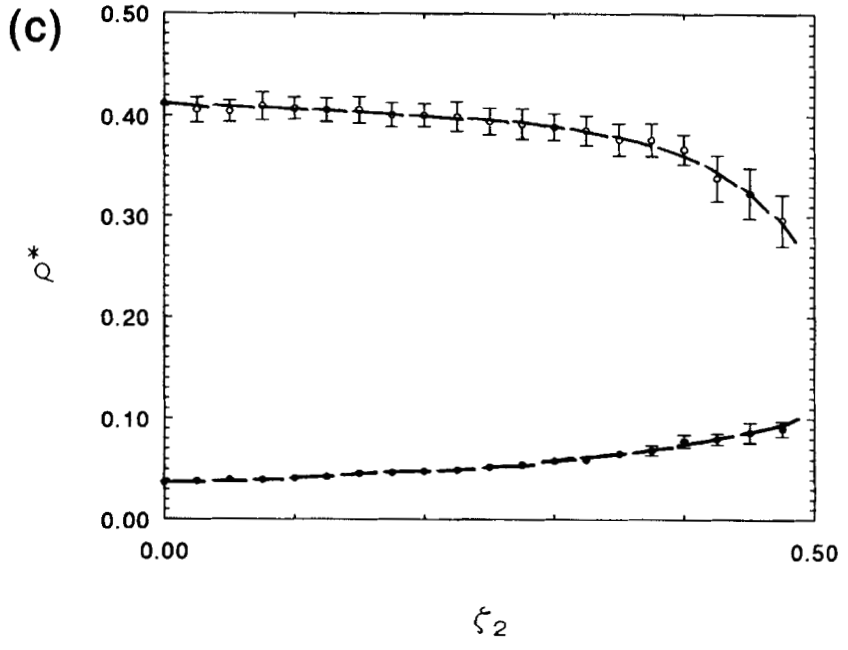

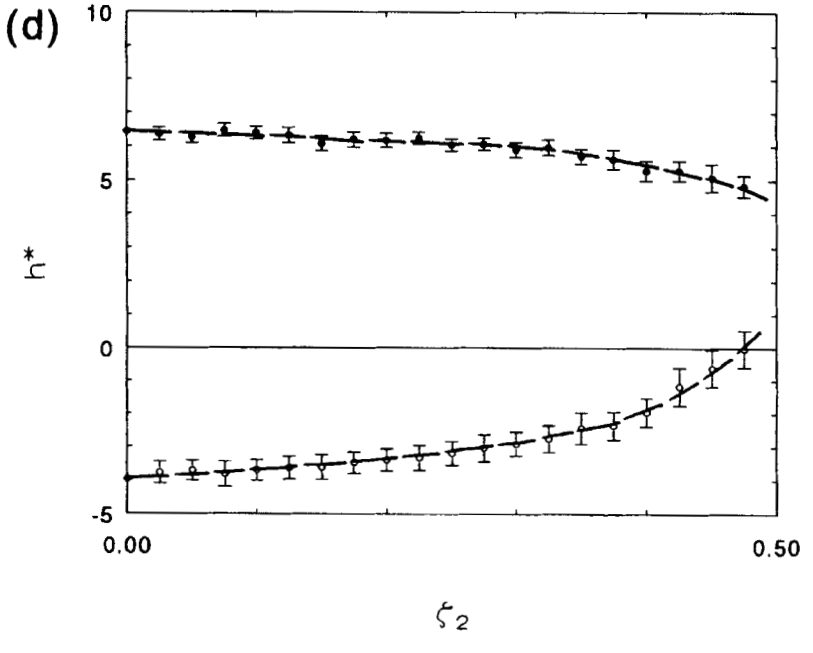

FIGURE 3

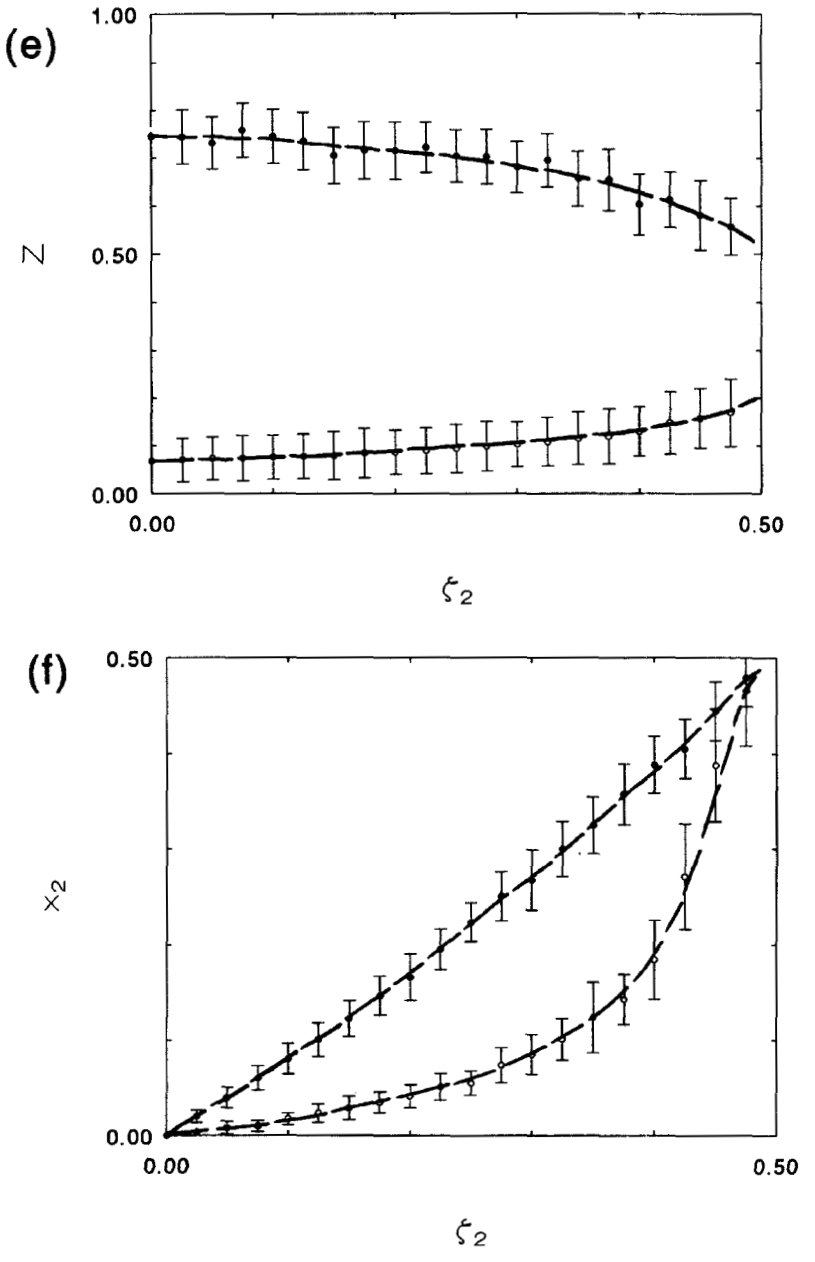

FIGURE 3 Vapour-liquid coexistence diagrams for mixture III at reduced temperature 2.35. (a) Pressure p^* as a function of fugacity fraction of species 2 ζ_2 (o: the Gibbs-Duhem integration path); (b) Pressure p^* as a function of mole fraction of species 2 ζ_2 (●: vapour boundary, o: liquid boundary); (c) Coexistence densities p^* as a function of fugacity fraction of species 2 ζ_2 (●: vapour boundary, o: liquid boundary); (d) Coexistence residual enthalpies h^* as a function of fugacity fraction of species 2 ζ_2 (●: vapour boundary, o: liquid boundary); (e) Coexistence compressibility factors Z as a funcction of fugacity fraction of species 2 ζ_2 (●: vapour boundary, o: liquid boundary); (f) Coexistence mole fraction x_2 as a function of fugacity fraction of species 2 ζ_2 (●: vapour boundary, o: liquid boundary). Error bars are included only if larger than the plot marks. Dashed lines on the phase boundaries are drawn only as a guide to the eye.

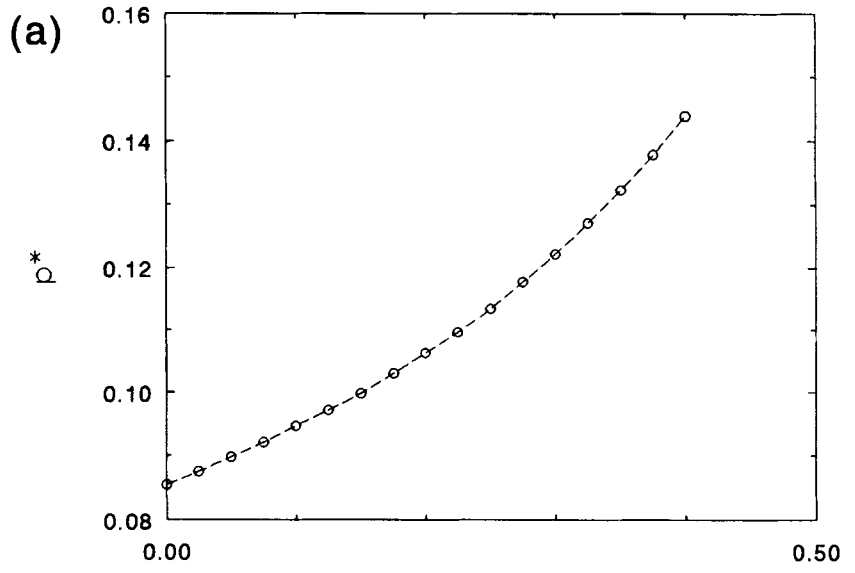

FIGURE 4 Vapour-liquid coexistence diagrams for mixture III at reduced temperature 2.45. (a) Pressure p^* as a function of fugacity fraction of species 2 ζ_2 (o: the Gibbs-Duhem integration path). (b) Pressure p^* as a function of mole fraction of species 2 x_2 (●: vapour boundary, o: liquid boundary). (c) Coexistence densities p^* as a function of fugacity fraction of species 2 ζ_2 (●: vapour boundary, o: liquid boundary); (d) Coexistence residual enthalpies h^* as a function of fugacity fraction of species 2 ζ_2 (●: vapour boundary, o: liquid boundary); (e) Coexistence compressibility factors Z as a function of fugacity fraction of species 2 ζ_2 (●: vapour boundary, o: liquid boundary); (f) Coexistence mole fraction x_2 as a function of fugacity fraction of species 2 ζ_2 (●: vapour boundary, o: liquid boundary). Error bars are included only in larger than the plot marks. Dashed lines on the phase boundaries are drawn only as a guide to the eye.

phases diminish and statistical errors increase. These facts are displayed in Figures 2c – f. Subsequently, the Gibbs-Duhem integration lost accuracy.

The components of mixture III are identical, but the cross-interaction energy parameter is weaker than the pure-component value. Hence, the pressure-composition diagram must be symmetrical. The plot of $p^* - \zeta_2$ and the pressure-composition diagram are displayed in Figure 3a, b. As $\zeta_2 = 0.50$ is approached, as in mixture II, differences in the properties of the two phases diminish and statistical errors increase. This is shown in Figures 3c – f. At $\zeta_2 = 0.50$, the differences were so small and statistical errors in the properties of the two phases were so large that the Gibbs-Duhem integration lost accuracy. This state point is close to the region of fluid-fluid immiscibility. As the temperature increases, these occur at lower values of ζ_2, namely at $\zeta_2 \sim 0.40$ for $T^* = 2.45$ and at $\zeta_2 \sim 0.33$ for $T^* = 2.55$. This is well demonstrated in Figures 4 and 5.

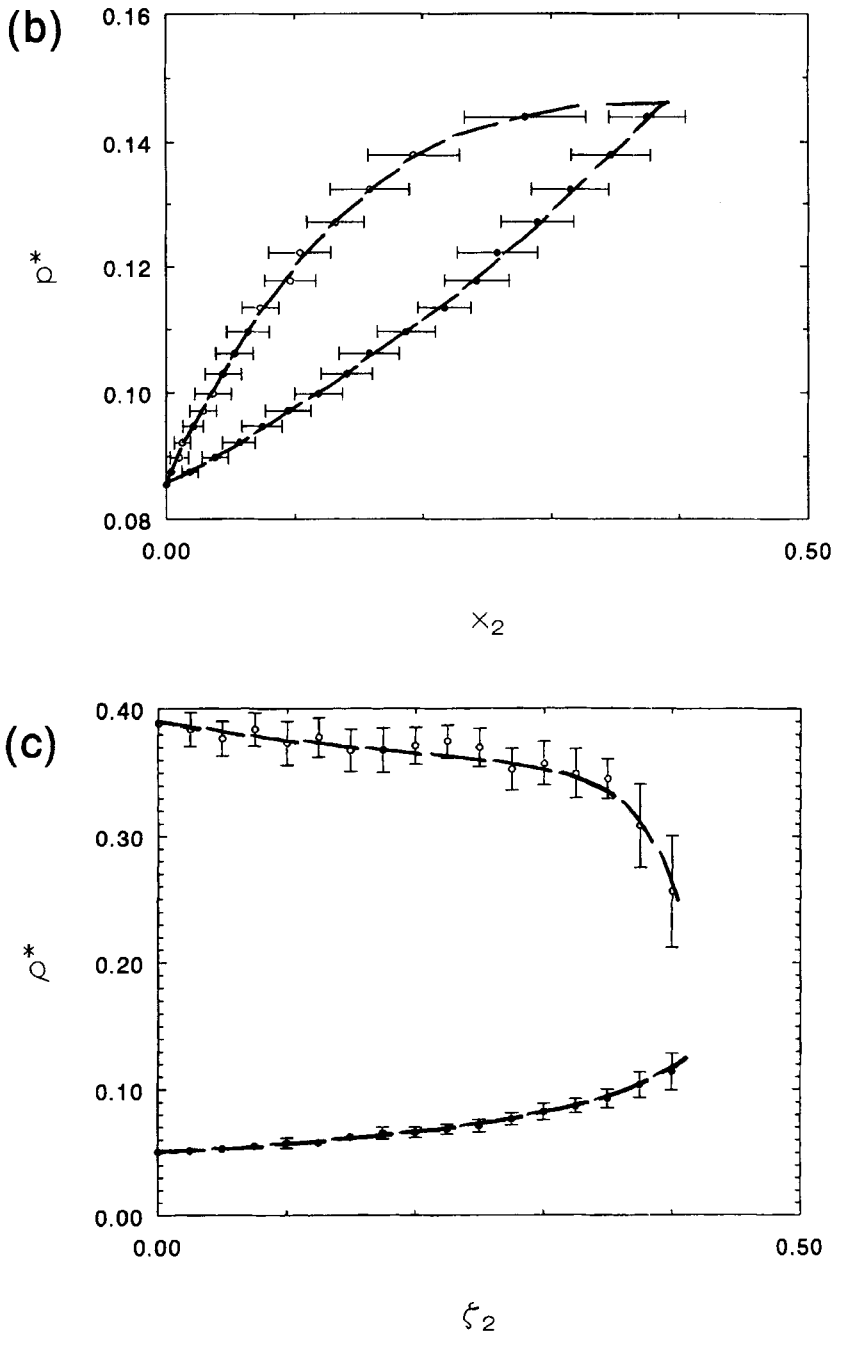

FIGURE 4

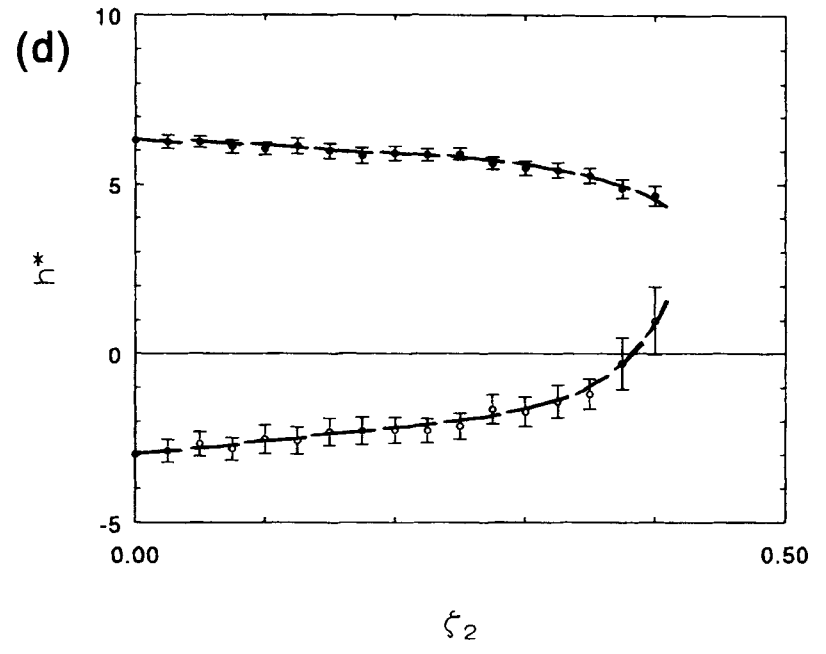

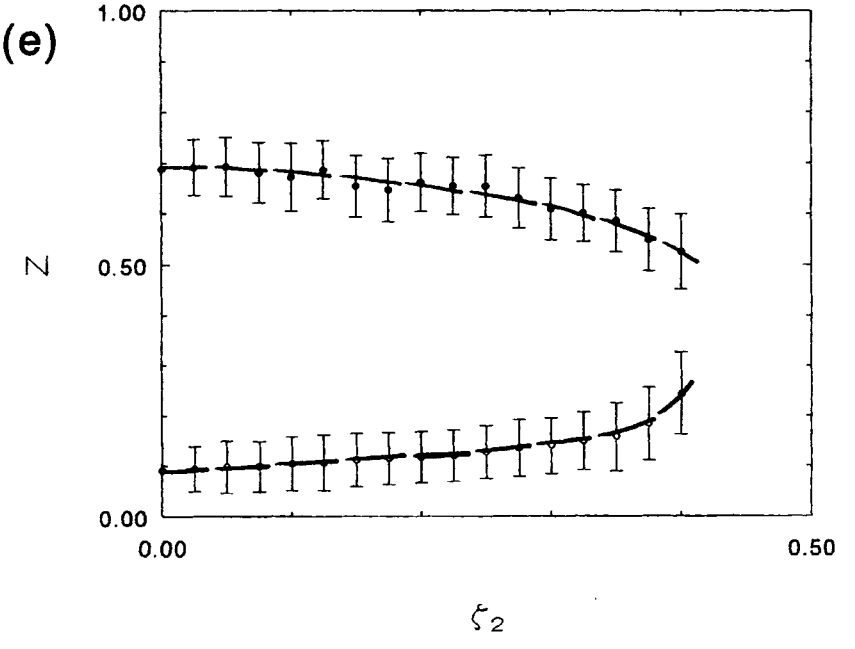

FIGURE 4

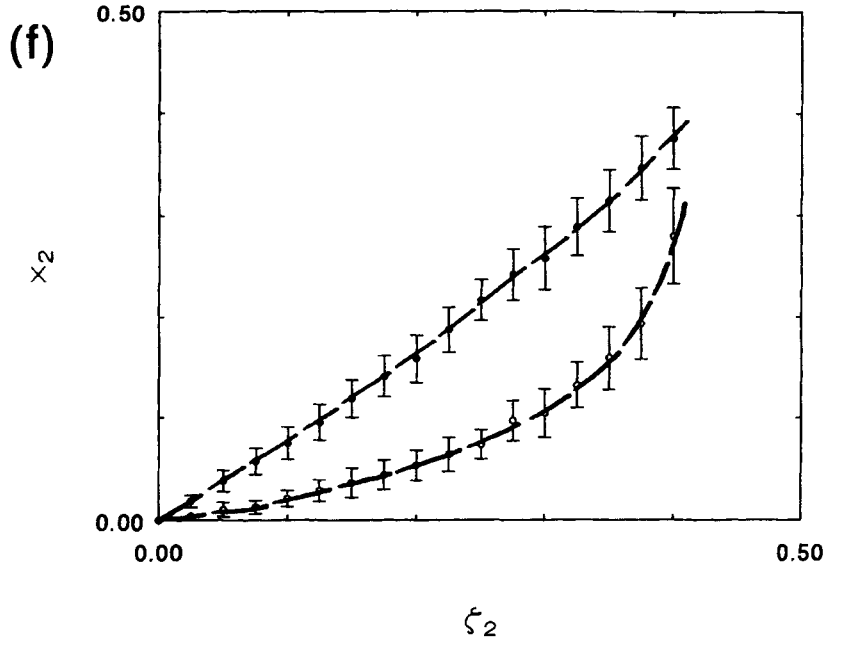

FIGURE 4

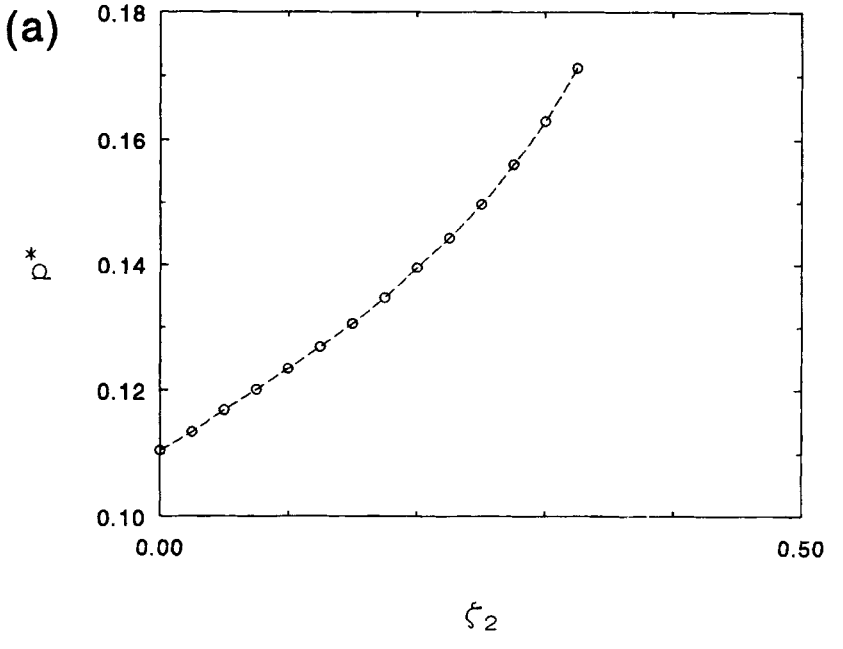

FIGURE 5

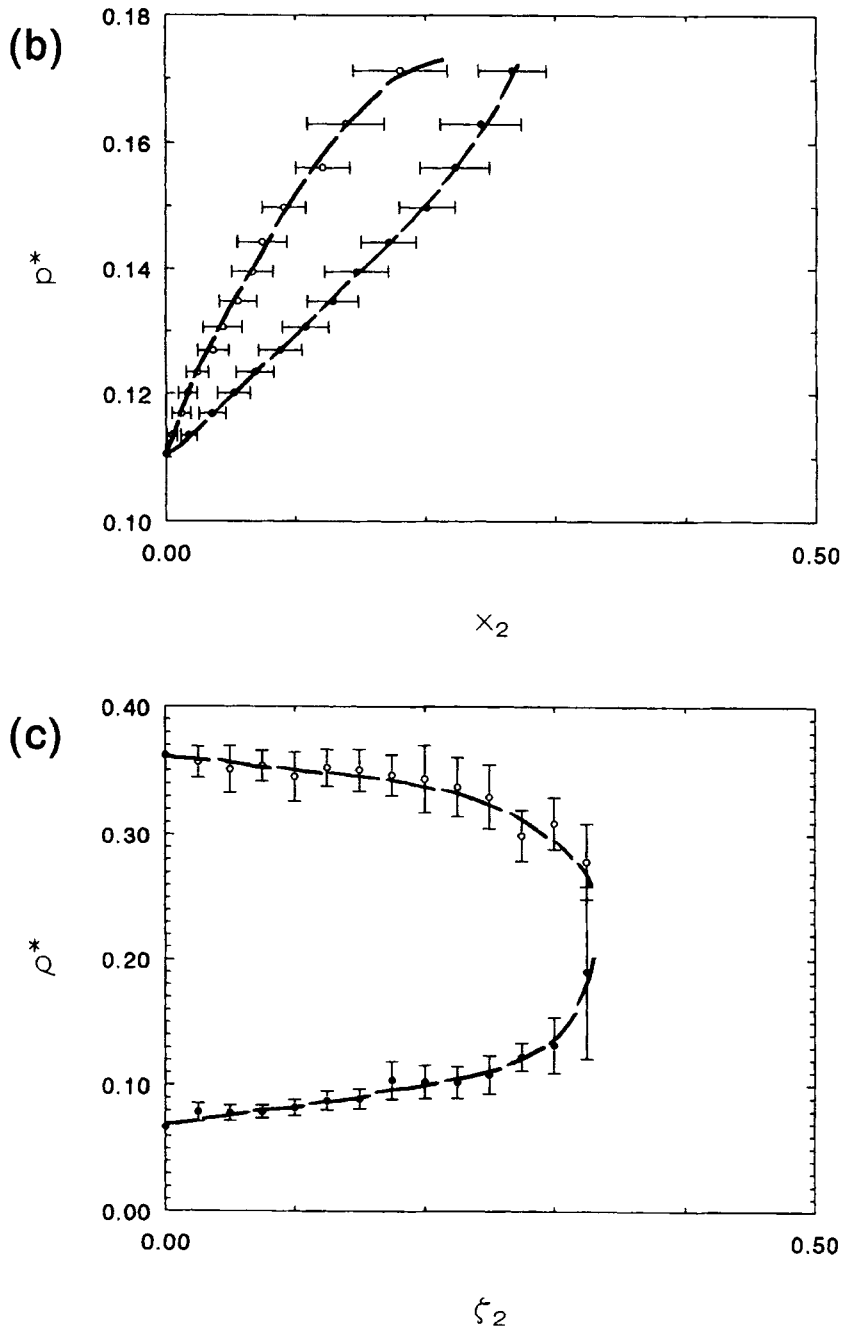

FIGURE 5

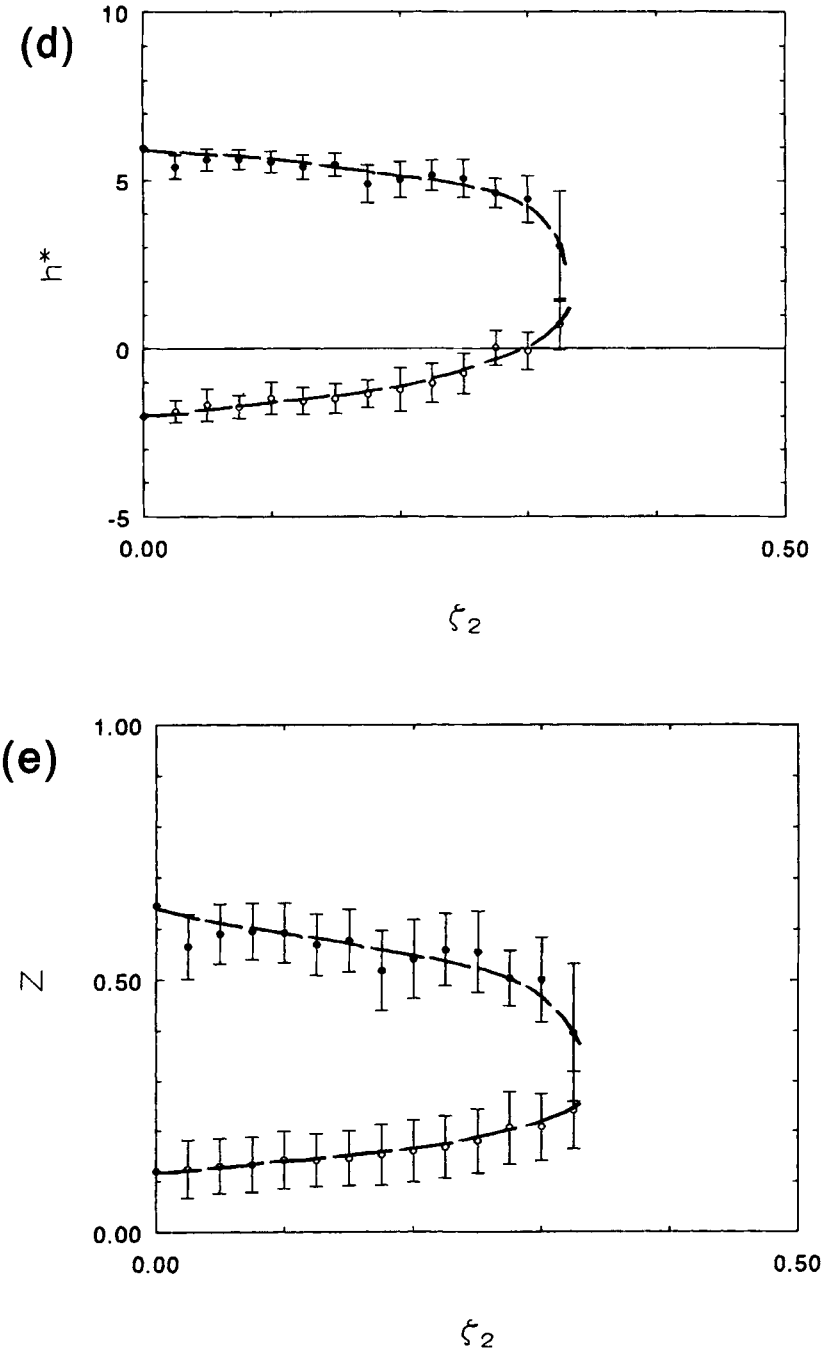

FIGURE 5

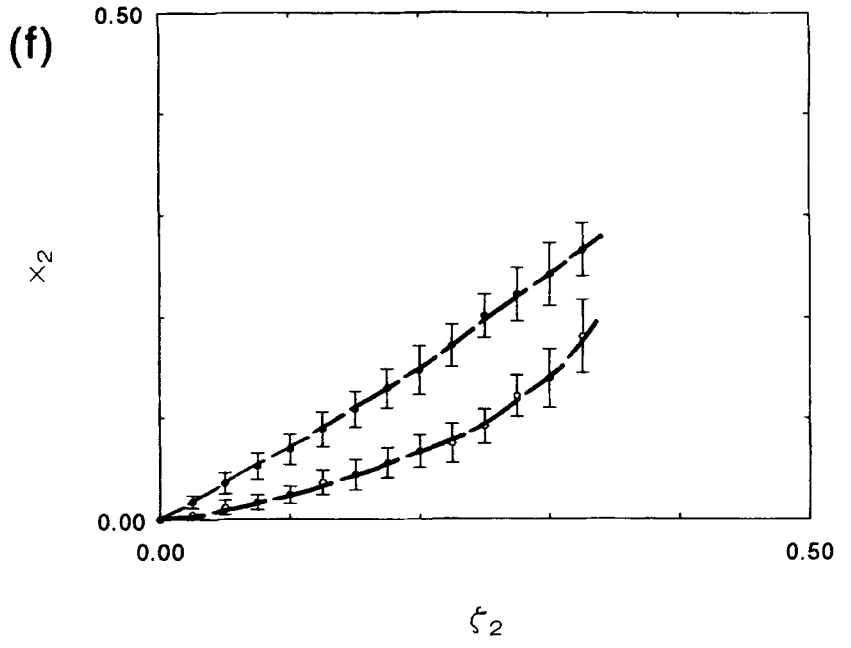

FIGUER 5 Vapour-liquid coexistence diagrams for mixture III at reduced temperature 2.55. (a) Pressure p^* as a function of fugacity fraction of species 2 ζ_2 (o: the Gibbs-duhem integration path); (b) Pressure p^* as a function of mole fraction of species 2 x_2 (●: vapour boundary, o: liquid boundary); (c) Coexistence densities p^* as a function of fugacity fraction of species 2 ζ_2 (●: vapour boundary, o: liquid boundary); (d) Coexistence residual enthalpies h^* as a function of fugacity fraction of species 2 ζ_2 (●: vapour boundary, o: liquid boundary); (e) Coexistence compressibility factors Z as a function of fugacity fraction of species 2 ξ_2 (●: vapour boundary, o: liquid boundary); (f) Coexistence mole fraction x_2 as a function of fugacity fraction of species 2 ζ_2 (●: vapour boundary, o: liquid boundary). Error bars are included only if larger than the plot marks. Dashed lines on the phase boundaries are drawn only as a guid to the eye.

5. CONCLUSIONS

We directly evaluated the vapour-liquid equilibria of molecular binary mixtures by MD simulations using the Gibbs-Duhem integration method [7]. The Gibbs-Duhem integration method, like the GEMC method, performed simultaneous but independent simulations of each phase. However, in contrast to the GEMC, the mechanism for equating the chemical potential (fugacity) of all components is the Clapeyron-type equation, which requires a change of species identity. Change of species identity works much more

efficiently than particle insertion. The Gibbs-Duhem integration method was applied to three prototypes of binary mixtures of 2CLJ fluids having elongations 0.3292, 0.505 and 0.67. The Gibbs-Duhem integration method loses accuracy as the transition weakens because differences in the properties of the two phases diminish and statistical errors increase. This also occurs in GEMC simulations, and this is due to the absence of an interface between the two regions in the two methods.

Acknowledgements

ML would like to acknowledge the partial support of the Grant Agency of the Academy of Sciences of the Czech Republic, grant No. 4721401. Calculations were made on the IBM SP2 in the IBM Computer Centre of the Czech Technical University and Institute of Chemical Technology, Prague.

References

[1] Panagiotopoulos, A. Z. (1992). "Direct determination of fluid phase equilibria by simulation in the Gibbs ensemble: A review", *Mol. Sim.*, **9**, 1–23.
[2] Panagiotopoulos, A. Z., Quirke, N., Stapleton, M., Tildesley, D. J. (1988). "Phase equilibria by simulation in the Gibbs ensemble. Alternative derivation, generalization and application to mixture and membrane equilibria", *Mol. Phys.*, **63**, 527–545.
[3] Allen, M. P. and Tildesley, D. J. (1987). *Computer Simulation of Liquids*, Clarendon Press.
[4] Strnad, M. and Nezbeda, I. (1996). "Extended Gibbs ensemble: A set of Gibbs ensembles with a fluctuating particle", *Mol. Sim.*, in press.
[5] Kofke, D. A. (1993). "Gibbs-Duhem integration: a new method for direct evaluation of phase coexistence by molecular simulation", *Mol. Phys.*, **78**, 1331–1336.
[6] Kofke, D. A. (1993). "Direct evaluation of phase coexistence by molecular simulation via integration along the saturation line", *J. Chem. Phys.*, **98**, 4149–4162.
[7] Mehta, M. and Kofke, D. A. (1994). "Coexistence diagrams of mixtures by molecular simulation", *chem. Eng. Sci.*, **49**, 2633–2645.
[8] Agrawal, R., Mehta, M. and Kofke, D. A. (1994). "Efficient evaluation of three-phase coexistence lines", *Int. J. of Thermophys.*, **15**, 1073–1083.
[9] Lisal, M. and Vacek, V. (1996). "Direct evaluation of vapour-liquid equilibria by molecular dynamics using Gibbs-Duhem integration", *Mol. Sim.*, **17**, 27–39.
[10] Kofke, D. A. and Glandt, E. D. (1988). "Monte Carlo of multicomponent equilibria in a semigrand ensemble", *Mol. Phys.*, **64**, 1105–1131.
[11] Kriebel, Ch., Müller, A., Winkelmann, J. and Fischer, J. (1995). "Vapour-liquid equilibria of two-centre Lennard-Jones fluids from the NpT plus test particle method", *Mol. Phys.*, **84**, 381–394.
[12] Denbigh, K. (1971). *Principles of Chemical Equilibrium*, Cambridge University Press, Cambridge.
[13] Berendsen, H. J. C., Postma, J. P. M., van Gunsteren, W. F., DiNola, A. and Haak, J. R. (1984). "Molecular dynamics with coupling to an external bath", *J. Chem. Phys.*, **81**, 3684–3690.
[14] Vega, L. F., Shing, K. S. and Rull, L. F. (1994). "A new algorithm for molecular dynamics simulations in the grand canonical ensemble", *Mol. Phys.*, **82**, 439–453.